Frascati Physics Series Vol. nnn (2001), pp. 000-000
Heavy Quarks at Fixed Target - Rio de Janeiro, Oct. 9-19, 2000

REVIEW OF EXPERIMENTAL RESULTS ON NEUTRAL B MESON OSCILLATIONS

Duccio ABBANEO
CERN, CH-1211, Geneva 23, Switzerland

ABSTRACT

The current status of the experimental knowledge of neutral B meson oscillations is reviewed.

The B^0_d oscillation frequency is precisely measured by SLD, CDF, and the LEP experiments. An overview of the analyses and their combination is presented. Preliminary measurements and perspectives at the running B factories are also briefly discussed.

The much faster B^0_s oscillations have not yet been resolved, despite the progress recently achieved by SLD and ALEPH. The world combination is presented, together with the expected and observed lower limit on the B^0_s oscillation frequency. The "amplitude method", used to combine the analyses in order to set the limit, is discussed also as a tool to establish the significance of a possible signal.

1 Introduction

One of the main goals of heavy flavour physics is to improve our knowledge of quark mixing and establish whether the Standard Model can describe precisely CP violating phenomena. Quark mixing is given by the CKM matrix, which can be written using the Wolfensteing parameterisation in terms of the three parameters λ, A, ρ and the CP violating phase η:

$$\begin{pmatrix} V_{ud} & V_{us} & V_{ub} \\ V_{cd} & V_{cs} & V_{cb} \\ V_{td} & V_{ts} & V_{tb} \end{pmatrix} \approx \begin{pmatrix} 1-\frac{1}{2}\lambda^2 & \lambda & A\lambda^3(\rho - i\eta) \\ -\lambda & 1-\frac{1}{2}\lambda^2 & A\lambda^2 \\ A\lambda^3(1-\rho-i\eta) & -A\lambda^2 & 1 \end{pmatrix} . \quad (1)$$

Neutral B meson oscillations are described by the "box diagrams" (Fig. 1). The oscillation frequency in the $B_d^0 - \overline{B_d^0}$ system, which is proportional to the

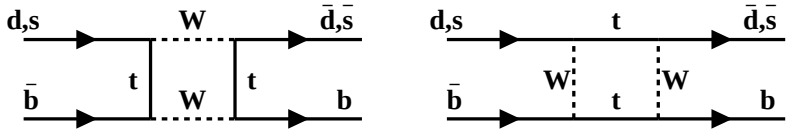

Figure 1: *Box diagrams giving rise to neutral B meson oscillations.*

mass difference of the two eigenstates, can be translated into a measurement of $\mid V_{td} \mid$, and therefore it yields information on the CP violating phase η (see Eq. 2). Unfortunately QCD effects are large and the associated uncertainty dominates the extraction of $\mid V_{td} \mid$.

$$\Delta m_d \propto \mid V_{td} \mid^2 \cdot \mathcal{F}(\mathrm{QCD}) \ . \quad (2)$$

A better constraint on η could be obtained from the ratio of the oscillation frequencies of B_s and B_d mesons, since some of the QCD uncertainties cancel in the ratio. The factor ξ in Eq. 3 is estimated to be known at the 5% level.

$$\frac{\Delta m_s}{\Delta m_d} = \frac{m_{B_s}}{m_{B_d}} \xi^2 \left| \frac{V_{ts}}{V_{td}} \right|^2 \ . \quad (3)$$

The proper time distributions of "mixed" and "unmixed" decays, given in Eq. 4, are measured experimentally. The oscillating term introduces a time-dependent difference between the two classes.

$$\begin{aligned} \mathcal{P}(t)_{B_q^0 \to \overline{B_q^0}} &= \frac{\Gamma e^{-\Gamma t}}{2} \left[1 - \cos(\Delta m_q \, t)\right] , \\ \mathcal{P}(t)_{B_q^0 \to B_q^0} &= \frac{\Gamma e^{-\Gamma t}}{2} \left[1 + \cos(\Delta m_q \, t)\right] , \end{aligned} \quad (4)$$

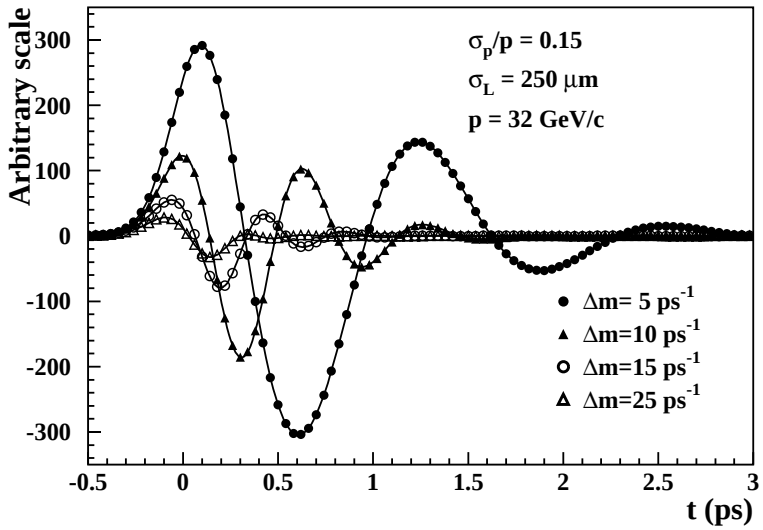

Figure 2: *Difference in the proper time distributions of unmixed and mixed decays for monochromatic B mesons, fixed decay length and momentum resolutions, and different values of the oscillation frequency.*

The amplitude of such difference is damped not only by the natural exponential decay, but also by the effect of the experimental resolution in the proper time determination. The proper time is derived from the measured decay length and the reconstructed momentum of the decaying meson. The resolution on the decay length σ_L is to first order independent of the decay length itself, and is largely determined by the tracking capabilities of the detector. The momentum resolution σ_p depends widely on the final state chosen for a given analysis, and is typically proportional to the momentum itself. The proper time resolution can be therefore written as:

$$\sigma_t = \frac{m}{p}\sigma_L \oplus \frac{\sigma_p}{p}\, t \ , \tag{5}$$

where the decay length resolution contributes a constant term, and the momentum resolution a term proportional to the proper time. Examples of the resulting difference are shown in Fig. 2, for the simple case of monochromatic B mesons of momentum 32 GeV/c, resolutions of $\sigma_p/p = 0.15$ and $\sigma_L = 250$ μm (Gaussian), and for different values of the true oscillation frequency. For low

frequency several periods can be observed. As the frequency increases, the effect of the finite proper time resolution becomes more relevant, inducing an overall decrease of observed difference, and a faster damping as a function of time (due to the momentum resolution component). In the example given for a frequency of 25 ps^{-1} only a small effect corresponding to the first half-period can be seen.

2 Analysis methods

The first step for a B meson oscillation analysis is the selection of final states suitable for the study. The choice of the selection criterion determines also the strategy for the tagging of the meson flavour at decay time. Then, the flavour at production time is tagged, to give the global mistag probability

Finally, the proper time is reconstructed for each meson candidate, and the oscillation is studied by means of a likelihood fit to the distributions of decays tagged as mixed or unmixed. The different selection methods and the techniques to tag the flavour at production time are briefly discussed below. Up-to-date references for all the Δm_d and Δm_s analyses can be found at

`http://lepbosc.web.cern.ch/LEPBOSC/`.

2.1 Selection methods

A variety of selection methods have been developed for B_d and B_s oscillation analyses, which offer different advantages in terms of statistics, signal purity and resolution.

Fully inclusive selections are used by SLD for both Δm_d and Δm_s analyses. At LEP they have been attempted by ALEPH for Δm_d and DELPHI for Δm_s. These methods yield very high statistics ($\mathcal{O}(10^5)$ decays at LEP, $\mathcal{O}(10^4)$ at SLD). The signal fraction is what is given by nature ($\approx 40\%$ for B_d and $\approx 10\%$ for B_s). There is no straightforward method for tagging the flavour at decay time. At LEP many different variables are combined by means of a neural network, while at SLD the excellent tracking capabilities allowed the development of the dipole technique, discussed later in Section 4.1.4.

Semi-inclusive selections rely on the identification of one specific B meson decay product. This is typically a lepton, (electron or muon), but it can be a fast kaon in the case of Δm_d analyses (used by SLD). The charge of this

particle gives the flavour at decay time, with small mistag probability. As for fully inclusive methods, there is no enhancement in signal fraction from the selection, and statistics are typically a factor of ten smaller. These methods are used by all experiments. In some cases an attempt is made to select a second B meson decay product in order to enhance the signal fraction. This is typically a "soft" pion from the decay $D^{\star +} \to D^0 \pi^+$ for Δm_d analyses, a kaon with charge opposite to the lepton, or a ϕ, in the case of Δm_s analyses.

In semi-exclusive selections the charmed meson from the B meson decay is fully reconstructed: a D or $D^\star$ for Δm_d analyses, a D_s for Δm_s analyses. The charmed meson reconstruction can be combined with the tagging of the lepton from the B meson decay, in which case only the neutrino is undetected. These methods have substantially lower statistics, but the signal purity goes up to 60% and the final state mistag probability is very small.

At LEP, ALEPH and DELPHI have also attempted full reconstruction of B_s decays. The selections yield only about 50 candidates, with $\approx 50\%$ estimated signal purity. Nevertheless, since all the decay products are identified, these events have excellent proper time resolution, and therefore give useful information in the high frequency range.

2.2 Flavour tagging at production time

All particles of the event except those tagged as the B meson decay products can be used to derive information on the B meson flavour at production time.

In the hemisphere containing the B meson candidate, charged particles originating from the primary vertex, produced in the hadronization of the b quark, may retain some memory of its charge. Either the charges of all tracks are combined, weighted according to the track kinematics, or the track closer in phase space to the B meson candidate is selected, requiring that it be compatible with a kaon for Δm_s analyses, with a pion for Δm_d analyses.

In the opposite hemisphere, the charge of the other b hadron can be tagged, exploiting the fact that b quarks are produced in pairs. Tracks from the b-hadron decay can be distinguished from fragmentation tracks on a statistical basis, from their compatibility with the primary vertex or with an inclusively-reconstructed secondary vertex. Inclusive hemisphere-charges can be formed assigning weights to tracks according to the probability that they belong to the primary or the secondary vertex, complemented with more "traditional"

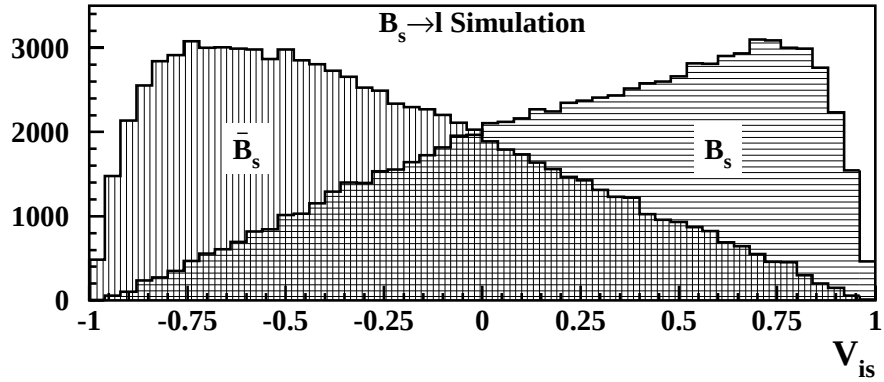

Figure 3: *Variable for flavour tagging at production time, for the inclusive lepton Δm_s analysis of ALEPH. Distribution of simulated signal events.*

jet-charges, where track weights are defined on the basis of track kinematics. Furthermore, specific decay products, such as leptons or kaons, can be searched for also in the opposite hemisphere, and their charge used as an estimator of the quark charge.

Finally, both at LEP and at SLD, the polar angle of the B meson candidate is also correlated with the charge of the quark, because of the forward-backward asymmetry in the Z decays. This correlation is particularly relevant at SLD, due to the polarisation of the electron beam.

Many of the production-flavour estimators mentioned above are correlated among themselves. The most recent and sophisticated analyses have attempted to use efficiently all the available information by combining the different estimators using neural network techniques. In Fig. 3 the combined initial state tag variable $V_{\rm is}$ is shown, for the case of the recent Δm_s analysis with inclusive lepton tag from ALEPH. The value of $V_{\rm is}$ is translated into a mistag probability, evaluated event-by-event. The lowest values for the production flavour mistag obtained at LEP are just below 25%, while at SLD values smaller than 15% are achieved. The difference is mostly due to the beam polarisation.

3 Measurements of $B_{\rm d}$ oscillations

A large number of analyses have been developed by SLD, CDF, and the LEP experiments, using the different selection techniques outlined in Section 2.1.

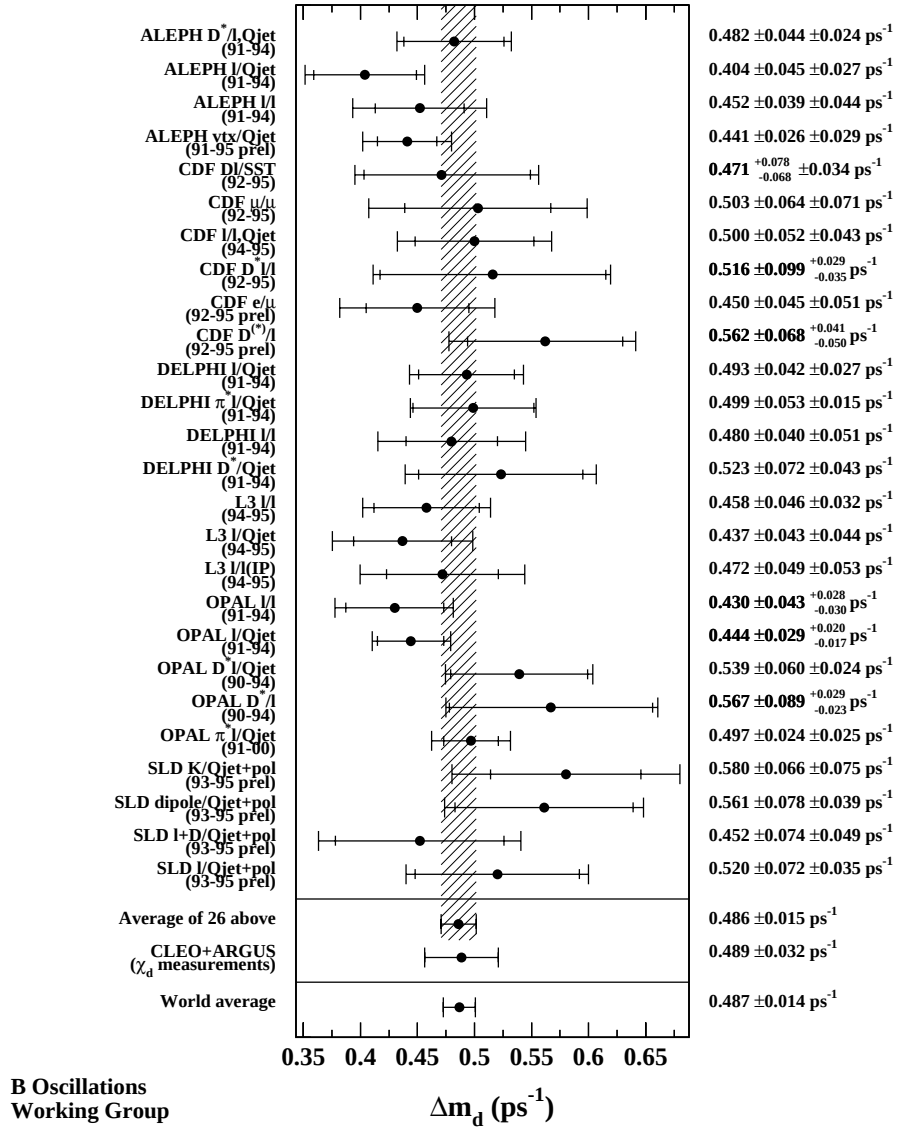

Figure 4: *Summary of Δm_d analyses from SLD, CDF, and the LEP experiments, together with the current world average (excluding asymmetric B factories).*

They are summarised in Fig. 4. One of the most recent and precise is the OPAL preliminary analysis based on inclusive reconstruction of B_d semileptonic decays. The selection aims at tagging $B_d \to D^{\star+}\ell^-\bar{\nu}$ decays, with $D^{\star+} \to D^0\pi_s^+$. The D^0 is reconstructed inclusively by selecting tracks and neutral objects compatible with the D^0 kinematics. The B_d decay vertex is reconstructed by intersecting the lepton with the soft pion. The neutrino energy is derived from the measured missing energy. The momentum resolution achieved is about 10%, with a mistag probability of about 28%. Combinations where the lepton and the soft pion have the same charge provide a useful control sample enriched in combinatorial background. The fraction of events tagged as mixed is dis-

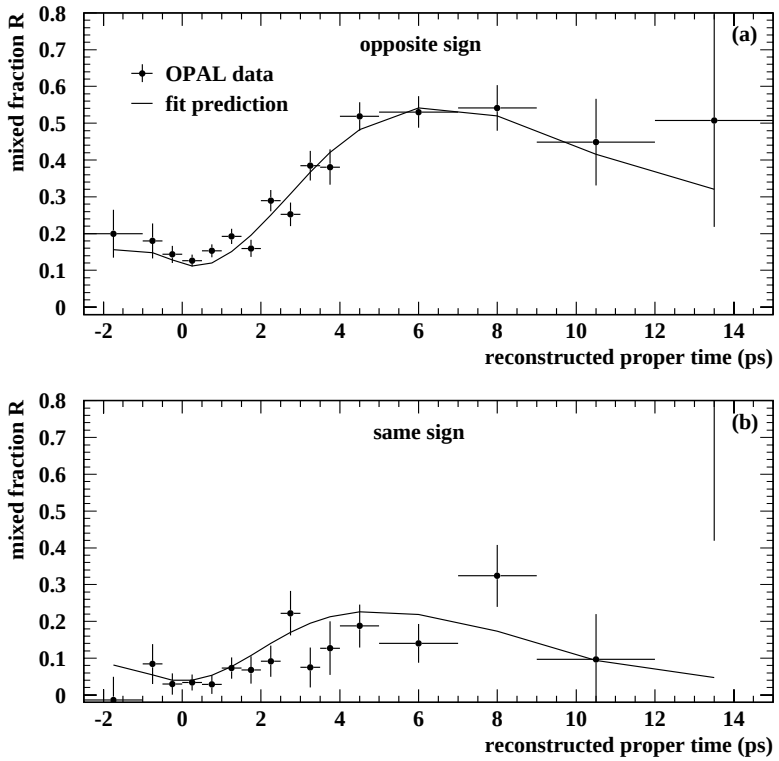

Figure 5: *Fraction of events tagged as mixed as a function of the reconstructed proper time, for the correct (a) and wrong (b) charge combinations. Superimposed is the curve predicted for the fitted value of* Δm_d.

played as a function of the reconstructed proper time in Fig. 5, for both charge combinations, together with the curve predicted for the fitted value of Δm_d. The analysis of all the available Z peak statistics, including those collected in the years 1996-2000 for the detector calibration, yields:

$$\Delta m_d = 0.497 \pm 0.024_{\rm stat} \pm 0.025_{\rm syst} \ \ {\rm ps}^{-1} \ . \tag{6}$$

3.1 The averaging method

All the Δm_d measurements reported in Fig. 4 require to some extent input from simulated events. Quantities derived from the simulation are affected by uncertainties on the physics processes that are simulated. These sources are common to all measurements, and they have to be treated as correlated when averaging individual results. Furthermore, in order to produce consistent measurements, and hence meaningful averages, the input physics parameters used in the simulation must be the same for all analyses in all experiments. For these reasons, all results are first adjusted to a common set of relevant input parameters, (*e.g.* b-hadron lifetimes and production fractions). Then results from SLD, CDF, and the LEP experiments are averaged, obtaining a first value for Δm_d. Following that, time-integrated measurements of χ_d from experiments at the Υ(4s) resonance are considered, and translated to Δm_d measurements. Measurements of the average time-integrated mixing parameter at the Z energy ($\bar{\chi} = f_{B_s}\chi_s + f_{B_d}\chi_d$) are also considered and translated to a constraint for the B_s production rate at the Z. This yields a new value of Δm_d and new b-hadron production fractions, which are used for a further iteration. The procedure is repeated until convergence.

The method yields a world average of Δm_d and consistent world average values for the b-hadron production fractions:

$$f_{B_d,B^+} = (40.0 \pm 1.0)\% \qquad f_{B_s} = (9.7 \pm 1.2)\% \qquad f_{\rm baryon} = (10.3 \pm 1.7)\% \ . \tag{7}$$

$$\Delta m_d = 0.487 \pm 0.014 \ {\rm ps}^{-1} \ . \tag{8}$$

3.2 The new results from the asymmetric B factories

New preliminary results from the asymmetric B factories have been made public this year. They are compared in Fig. 6 to the averages of the other experiments. The two BaBar results should not be averaged since they have some

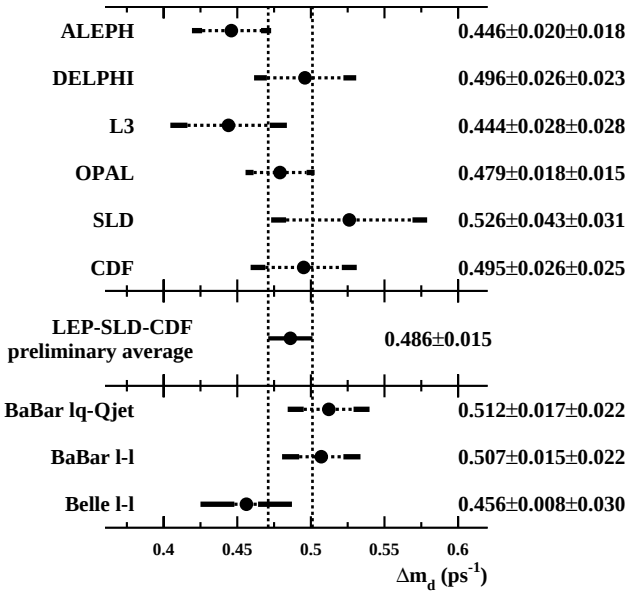

Figure 6: *Δm_d averages from SLD, CDF, and the LEP experiments, compared to the new results from the asymmetric B factories.*

statistical and systematic correlation that has not been estimated. The asymmetric B factories have already exceeded the statistical precision of the world average. At the moment they are quoting rather large systematic errors, which are however dominated by uncertainties on parameters that are also measured in their data. Therefore the large statistics expected in the near future will allow very precise measurements to be made.

4 Studies of B_s oscillations

The analyses completed so far are not able to resolve the fast B_s oscillations: they can only exclude a certain range of frequencies. Combining such excluded ranges is not straightforward, and a specific method, called "amplitude method" has been introduced for this purpose [1]. In the likelihood fit to the proper time distribution of decays tagged as mixed or unmixed, the frequency of the oscillation is not taken to be the free parameter, but it is instead fixed to a "test" value ω. An auxiliary parameter, the amplitude $\mathcal{A}$ of the oscillat-

ing term is introduced, and left free in the fit. The proper time distributions for unmixed and unmixed decay, prior to convolution with the experimental resolution, are therefore written as

$$\mathcal{P}(t) = \frac{\Gamma e^{-\Gamma t}}{2} \left[1 \pm \mathcal{A} \cos(\omega\, t)\right] , \tag{9}$$

with ω the test frequency and $\mathcal{A}$ the only free parameter. When the test frequency is much smaller than the true frequency ($\omega \ll \Delta m_s$) the expected value for the amplitude is $\mathcal{A} = 0$. At the true frequency ($\omega = \Delta m_s$) the expectation is $\mathcal{A} = 1$. All the values of the test frequency ω for which $\mathcal{A} + 1.645\sigma_{\mathcal{A}} < 1$ are excluded at 95% C.L.

The amplitude has well-behaved errors, and different measurements can be combined in a straightforward way, by averaging the amplitude measured at different test frequencies. The excluded range is derived from the combined amplitude scan.

4.1 Examples of Δm_s analyses

Some examples of recent and relevant analyses are presented in the following, and their statistical power discussed and compared.

4.1.1 Exclusive B_s reconstruction at LEP

Analyses of fully reconstructed B_s candidates have been performed by ALEPH and DELPHI, exploiting the decay channels $B_s^0 \to D_s^{(\star)-}\pi^+$ and $B_s^0 \to D_s^{(\star)-}a_1^+$. DELPHI also uses $B_s^0 \to \overline{D^0}K^-\pi^+$ and $B_s^0 \to \overline{D^0}K^-a_1^+$. The reconstructed mass structure consists of a narrow peak at the nominal B_s mass plus a broad shoulder at lower masses due to the decays involving a $D_s^\star \to D_s\gamma$ with the photon undetected (see Fig. 7).

The signal purity is $\approx 50\%$, with a proper time resolution of $\sigma_t \approx 0.08$ ps, to be compared with $\sigma_t \approx 0.2 \div 0.3$ ps for the other analyses at LEP.

4.1.2 Analyses of $D_s^-\ell^+$ final states at LEP

At LEP, these methods represent a good compromise between statistics, signal purity and resolution.

The signal purity achieved is typically around or above 50%, with about 40% combinatorial background and 10% physical background from $B \to D_s\bar{D}$

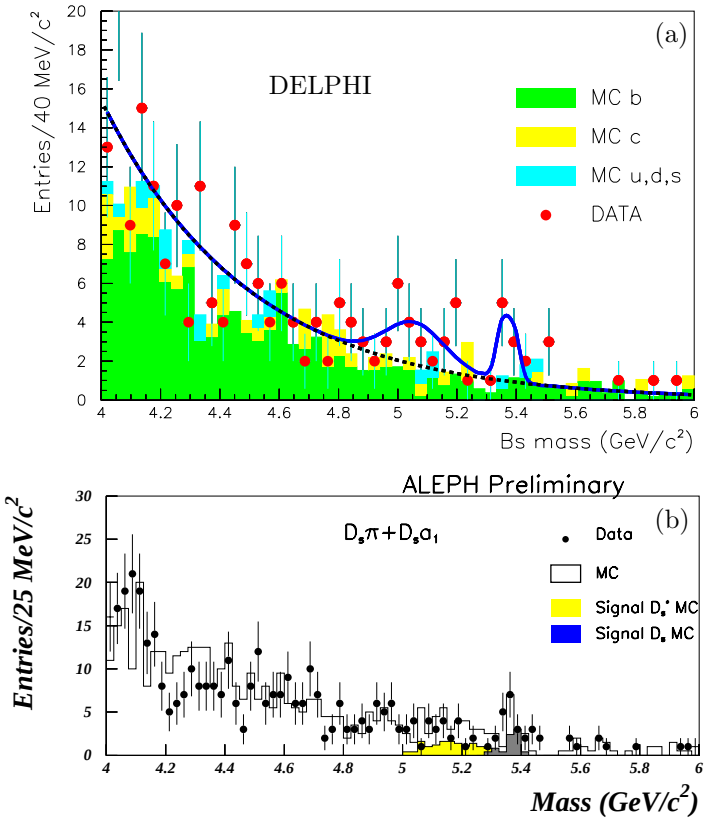

Figure 7: *Reconstructed B_s mass in DELPHI (a) and ALEPH (b).*

decays, with $\bar{D} \to \ell^- \bar{\nu} X$. The combinatorial background is controlled from the data using the D_s mass peak sidebands (see Fig. 8). The decay length resolution is ≈ 200 μm and the momentum resolution about 10% due to the undetected neutrino, whose momentum is derived from the measured missing energy. Statistics are typically a few hundred candidates.

4.1.3 Analyses of inclusive lepton samples at LEP and SLD

These analyses give the highest sensitivity both at LEP and at SLD. Lepton candidates from direct b-hadron decays are selected on the basis of the lepton kinematics; non-b background is suppressed by applying lifetime-based b

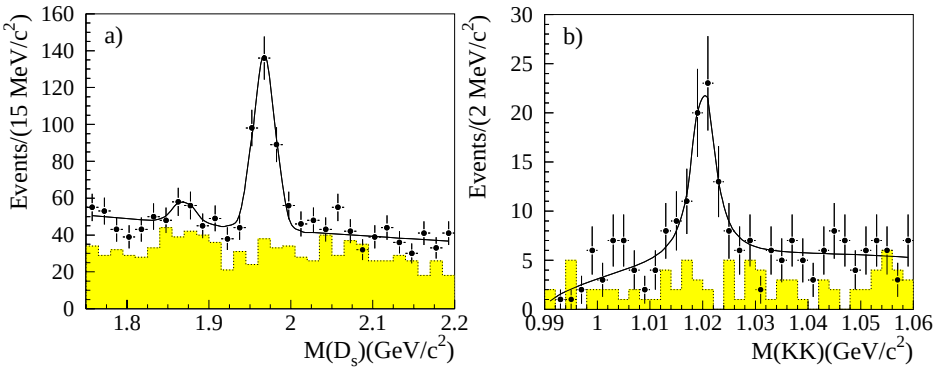

Figure 8: *Reconstructed D_s mass peak for the DELPHI $D_s^-\ell^+$ analysis, for the fully hadronic D_s decay channels (a). For the same analysis, ϕ mass peak for the $D_s^- \to \phi\ell^-$ channel (b).*

tagging algorithms. The charmed particle is reconstructed inclusively and intersected with the lepton to find the b decay vertex. At LEP, the resolution has typically a core of 250 μm with tails up to 1 mm, worse than for $D_s\ell$ final states, due to the contribution of missing or misassigned tracks. At SLD, the small and precise CCD vertex detector allows a core resolution of about 60 μm to be achieved. The neutrino momentum is estimated from the missing energy, with resolution similar to the $D_s\ell$ case.

The sensitivity of the analysis can be further improved by estimating the probability that each event be signal, instead of using the average B_s fraction (about 10%). The total charge flowing out of the b vertex is a good discriminant between B^+ and neutral b hadrons. The presence of kaons from the primary vertex, or among the tracks assigned to the c meson, can discriminate between B_s mesons and other b hadrons. Such information can be combined into a single discriminating variable (see Fig. 9) and the signal fraction evaluated event by event, as a function of such variable. This procedure enhances the statistical power of the analyses by up to 25%.

4.1.4 The fully inclusive analysis at SLD

In a fully inclusive analysis, both the c and the b decay vertices are reconstructed topologically. This requires excellent tracking capabilities, to keep the contribution of missing or misassigned tracks at an acceptable level. The

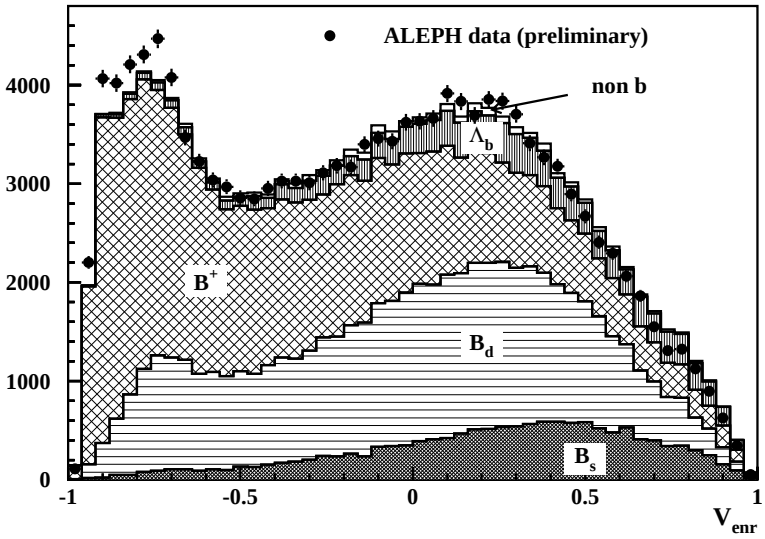

Figure 9: *Variable discriminating B_s decays from other b hadrons, for the inclusive lepton Δm_s analysis of ALEPH. The signal fraction is evaluated event-by-event as a function to such a variable.*

method is particularly suitable for SLD, where the available statistics are ten times smaller than in a LEP experiment, but with much more precise tracking.

Since no specific b decay product is tagged, the flavour at decay time has to be identified with a dedicated method. SLD takes advantage of the good separation between the B and the D meson vertices to build a variable which measures the "charge flow" between the two, ("charge dipole") which exploits the fact that a B_s meson decays to a D_s^- meson, while a $\overline{B_s}$ decays to a D_s^+. The kind of separation achieved can be seen in Fig. 10.

The statistics collected are four times larger than for the inclusive lepton analysis, which compensates for the slightly worse decay length resolution (core of ≈ 70 μm) and the larger dilution in the flavour tag at decay time, yielding a very similar statistical power.

4.1.5 Comparison of analyses

The available $D_s\ell$ and inclusive lepton analyses at LEP are compared in Fig. 11, for what concerns their statistical power.

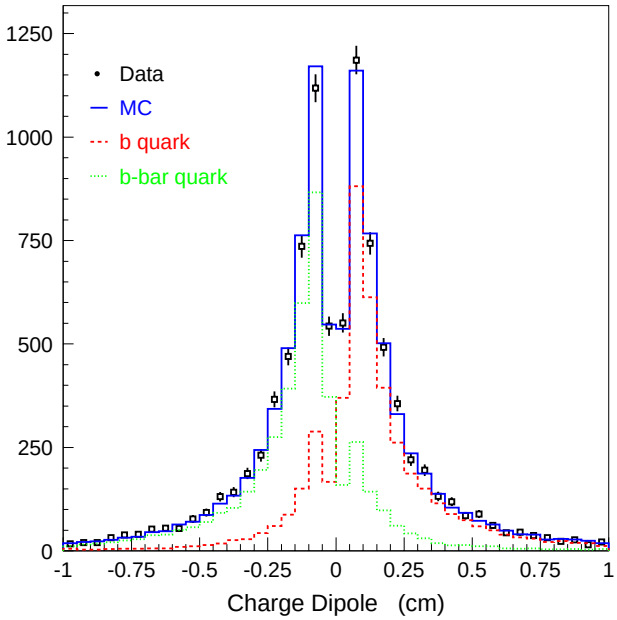

Figure 10: *Flavour tag at decay time for the fully inclusive analysis of SLD.*

A striking feature is that the $D_s\ell$ analysis from DELPHI has a slightly smaller statistical error than the ALEPH one at low frequency, but it becomes much worse at high frequency (the statistical error is larger by more than a factor of two). Similarly the slope of the error curve for the ALEPH inclusive lepton analysis is substantially more flat than for DELPHI.

A plausible reason for that is demonstrated in Fig. 12a, where the ALEPH inclusive lepton analysis is compared with the same analysis if the event-by-event treatment of the decay length bias correction and error assignment is dropped. In the analysis the decay length is reconstructed by intersecting the charm meson candidate direction with the lepton track, and its uncertainty is estimated from the fit error. The fitted decay length needs to be corrected for a small bias caused by the selection (bias correction), and the fit error must be enlarged to account for the contribution of missing or misassigned tracks (pull correction). These corrections, taken from the simulation, depend strongly on the event topology: they are negligible for well measured decays where the charmed meson is almost fully reconstructed, they can be very large in

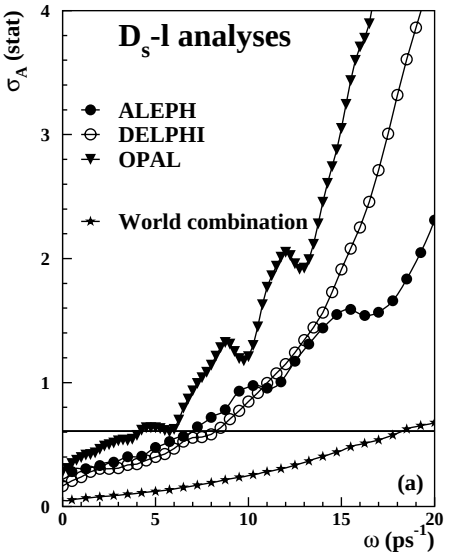

Figure 11: *Statistical error on the measured amplitude as a function of test frequency for the analyses of $D_s\ell$ final states (a) and inclusive lepton samples (b) at LEP. The world combination of all analyses is shown for comparison.*

other cases. Parametrising carefully such corrections as a function of the event topology is mandatory to achieve a good sensitivity at high frequency. That is valid, to some extent, also for $D_s\ell$ analyses, although the variety of topologies is more limited. These considerations suggest that a big factor could still be gained in the statistical power of the DELPHI analyses at high frequency[1].

In Fig. 12b, the two best analyses from SLD, the inclusive lepton and fully inclusive analyses, are compared with the corresponding best available at LEP. Compared to the ALEPH analysis, the SLD inclusive lepton analysis at low frequency has errors larger by more than a factor of two, due to the smaller statistics, only partially compensated by the better flavour tag at production time (see Section 4.1.3). As the frequency increases, the decay length resolution becomes more and more relevant, and the two analyses become eventually equivalent.

[1]In the DELPHI $D_s\ell$ analysis the fit error is not used to estimate event-by-event the decay length uncertainty: the average resolution is taken instead.

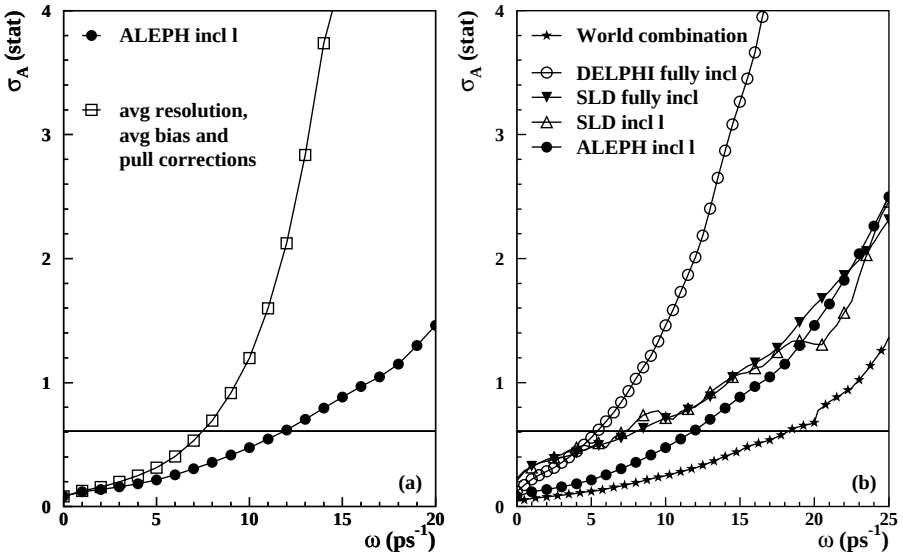

Figure 12: *(a) Comparison of the statistical errors on the amplitude for the ALEPH inclusive lepton analysis, with the same analysis if the event-by-event treatment of bias and pull corrections and decay length uncertainty is dropped. (b) Comparison of the SLD inclusive lepton and fully inclusive analyses, with the corresponding best available at LEP.*

The comparison of the SLD and DELPHI fully inclusive analyses shows the difficulty of such a method at LEP.

In Fig. 13 the combinations of the analyses from each experiment are compared. At high frequency the world combination is dominated by SLD and ALEPH.

4.2 Results from the world combination

The amplitude spectrum for the world combination, with statistical and systematic errors is shown in Fig. 14. A lower limit of $\Delta m_s > 15.0$ ps^{-1} is derived, while the expected limit (sensitivity) is $\Delta m_s > 18.0$ ps^{-1}. The difference is due to the positive amplitude values measured around 17 ps^{-1}, compatible with one, as expected in the presence of signal. The error on the amplitude at high frequency ($\Delta m_s \approx 20$ ps^{-1}) is reduced by about a factor of two compared to the world combination of Summer 1999, mostly because of the progress of the

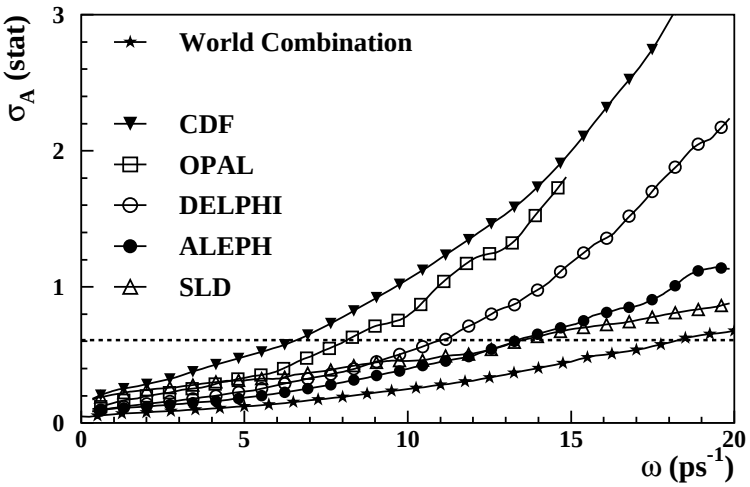

Figure 13: *Comparison of the statistical errors on the amplitude for the combination of analyses experiment by experiment. At high frequency the world average is dominated by SLD and ALEPH.*

SLD and ALEPH analyses.

The amplitude spectrum can be translated to a likelihood profile, referred to the asymptotic value for $\Delta m_s \to \infty$ (see Fig.15). A minimum is observed at $\Delta m_s \approx 17$ ps^{-1}. The deviation of the measured amplitude from $\mathcal{A} = 0$ around the likelihood minimum is about 2.4σ. Such a value cannot be used to assess the probability of a fluctuation, since it is chosen *a posteriori* among all the points of the frequency scan performed. On the other hand because the amplitude measurements at different frequencies are correlated, the probability of observing a minimum as or more incompatible with the hypothesis of background than the one found in the data, needs to be estimated with toy experiments [2)]. Such a probability is found to be about 3%.

An interesting issue is to which extent the observation is compatible with the hypothesis of signal. This cannot be assessed quantitatively in a non-trivial way. In Fig. 16 the expected amplitude shapes, calculated analytically [2)], are shown for the simple case of monochromatic B_s mesons of $p = 32$ GeV/c which oscillates with a frequency of 17 ps^{-1}, with different (Gaussian) resolutions in momentum and decay length. The shapes are largely different; the only solid features are that the expectation is $\mathcal{A} = 1$ at the true frequency and $\mathcal{A} = 0$ far

below the true frequency.

In the world combination many analyses contribute, which have very different momentum and decay length resolution. In the most sensitive analyses, even, each event enters with its specific estimated resolutions, therefore contributing with a different expected amplitude shape. Calculating the expected amplitude shape for the world combination in the hypothesis of signal is therefore, at the moment, completely impractical.

It can certainly be stated, however, that qualitatively the shape observed in Fig. 14 is well compatible with the hypothesis of a signal at $\Delta m_s \approx 17$ ps^{-1}.

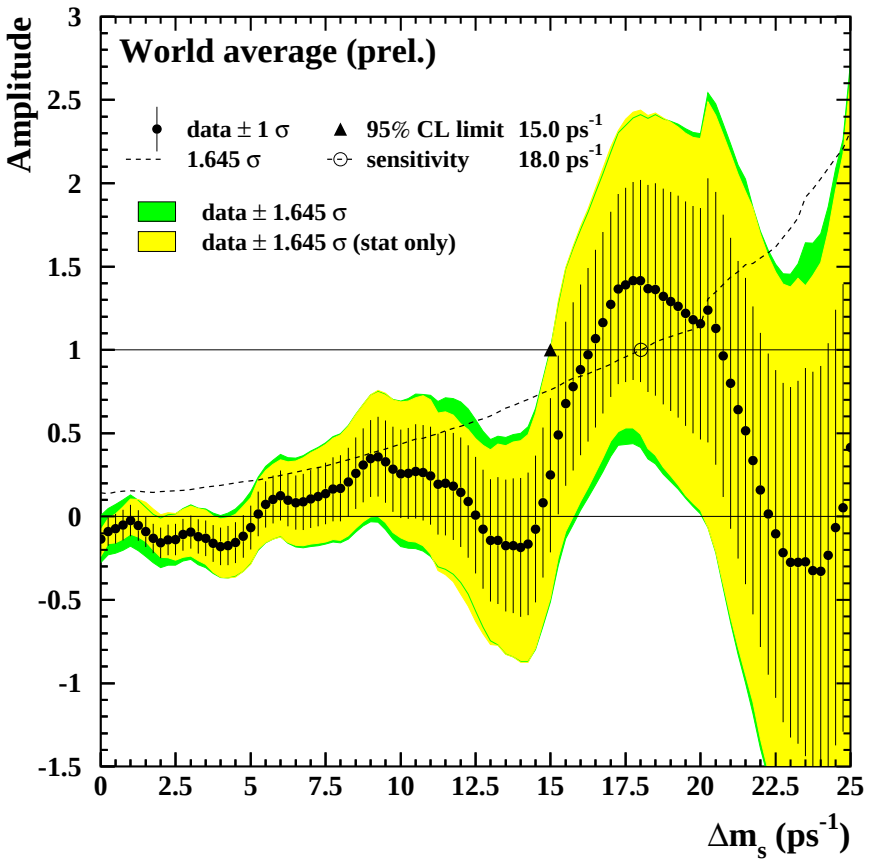

Figure 14: *Measured amplitude as a function of test frequency for the world combination.*

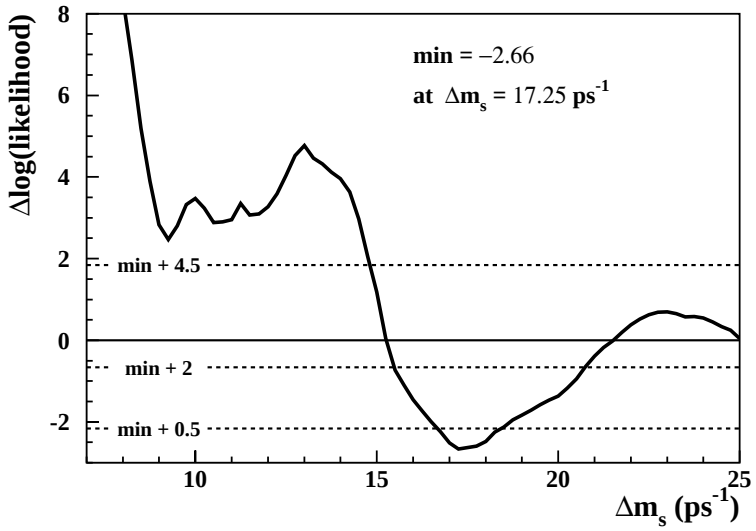

Figure 15: *Likelihood profile as derived from the amplitude spectrum (world combination). The dashed lines would represent the* $1-2-3$ σ *levels, if the likelihood was parabolic in a range wide enough around the minimum.*

4.3 Indirect constraints

Indirect constraints on Δm_s can be derived, within the Standard Model framework, from other physics quantities.

Measurements of charmless b decays, CP violation in the kaon system, and B meson oscillations can all be translated, with nontrivial theoretical input, to constraints on the (ρ, η) parameters [3], and combined, as shown in Fig. 17a. If the limit on Δm_s is removed from the fit, a probability density function can be extracted from the other parameters, shown in Fig. 17b. The preferred value is $\Delta m_s = 14.9^{+4.0}_{-3.6}$ ps^{-1}, perfectly compatible with the indication observed in the combination of Δm_s analyses.

The present world average of the width difference in the B_s system [4], $\Delta\Gamma_s/\Gamma_s = 0.16\,^{+0.08}_{-0.09}$, can be also translated to a value for the oscillation frequency, using the prediction of NLO+lattice calculations [5] for the ratio $\Delta\Gamma_s/\Delta m_s$. That gives $\Delta m_s = 16\,^{+8}_{-9} \pm 5$ ps^{-1}, very similar to the previous result, but with larger errors.

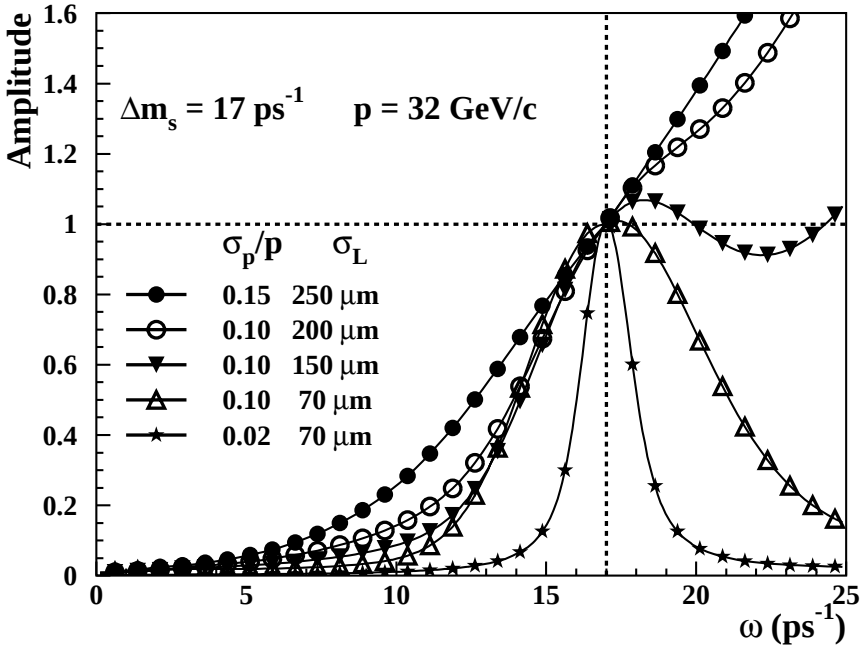

Figure 16: *Expected amplitude shape for a true frequency* $\Delta m_s = 17$ ps^{-1}, *monochromatic* B_s *mesons of* $p = 32$ GeV/c *and different values of momentum and decay length resolutions (taken to be Gaussian).*

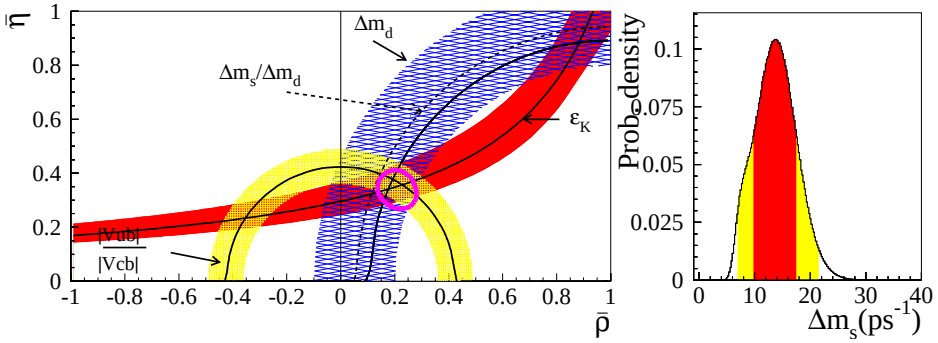

Figure 17: *Constraints in the* (ρ, η) *plane from charmless b decays, CP violation in the kaon system, and B meson oscillations (a). Constraint on the* Δm_s *derived from the fit with the* B_s *oscillation information removed (b).*

5 Conclusions

The B_d oscillation frequency has been precisely measured by CDF, SLD and the LEP eperiments:

$$\Delta m_d = 0.497 \pm 0.014 \text{ ps}^{-1} \ . \tag{10}$$

Asymmetric B factories will soon improve substantially on such result.

B_s oscillations are not yet resolved. A lower limit is set

$$\Delta m_s > 15.0 \text{ ps}^{-1} \qquad @ \ 95\% \text{ C.L.} \ . \tag{11}$$

The expected limit is 18.0 ps^{-1}, the difference being due to a deviation of about 2.4σ from $\mathcal{A} = 0$ observed for frequencies around 17 ps^{-1}. The deviation is qualitatively compatible with the pattern expected for a signal. The probability that it be due to a fluctuation is estimated to be about 3%.

6 Acknowledgements

I wish to thank the organisers of the Conference for inviting me, and in particular Alberto Reis, amicable host. I am grateful to Gaëlle Boix and Achille Stocchi, who provided several plots and numbers.

References

1. H.G. Moser and A. Roussarie, Nucl. Instrum. Methods A **384**, 491 (1997).
2. D. Abbaneo and G. Boix, JHEP **08**, 004 (1999).
3. F. Parodi, P. Roudeau, A. Stocchi, Il Nuovo Cimento **Vol. 112 A**, N. 8 (1999)
4. ALEPH, CDF, DELPHI, L3, OPAL, SLD, Combined results on b-hadron production rates, lifetimes, oscillations and semileptonic decays, CERN EP/2000-096.
5. M.Beneke, private communication updating M.Beneke *et al*, Phys. Lett. B **459**, 631 (1999), with lattice calculations of S. Hashimoto, hep-lat/9909136, KEK-CP093 (1999).